Systems & Control Transactions

Research Article
Foundations of Computer Aided Process Design (FOCAPD 2024)
Breckenridge, Colorado, USA. July 14-18, 2024
Peer Reviewed Conference Proceeding

PSE PRESS

Constraint Formulations for Bayesian Optimization of Process Simulations: General Approach and Application to Post-Combustion Carbon Capture

Clinton M. Duewall[ab]*, Mahmoud M. El-Halwagi[a]

[a] Texas A&M University, Artie McFerrin Department of Chemical Engineering, College Station, TX, USA
[b] Bryan Research & Engineering, LLC, Bryan, TX, USA
* Corresponding Author: clint.duewall@bre.com.

ABSTRACT

Some of the most highly trusted and ubiquitous process simulators have solution methods that are incompatible with algorithms designed for equation-oriented optimization. The natively unconstrained Efficient Global Optimization (EGO) algorithm approximates a black-box simulation with kriging surrogate models to convert the simulation results into a reduced-order model more suitable for optimization. This work evaluates several established constraint-handling approaches for EGO to compare their accuracy, computational efficiency, and reliability using an example simulation of an amine post-combustion carbon capture process. While each approach returned a feasible operating point in the number of iterations provided, none of them effectively converged to a solution, exploring the search space without effectively exploiting promising regions. Using the product of expected improvement and probability of feasibility as next point selection criteria resulted in the best solution value and reliability. Constraining probability of feasibility while solving for the next sample point was the least likely to solve, but the solutions found were most likely to be feasible operating points.

Keywords: Derivative Free Optimization, Surrogate Modeling, Process Simulation, Global optimization, Carbon Capture.

INTRODUCTION

Process simulators are trusted sources of property prediction and process design calculations [1]. Some process simulations have characteristics that challenge most optimization algorithms. Black-box simulators have no exploitable functional form, computationally expensive executions, and approximate derivatives. Coupled with highly constrained optimization formulations, these characteristics make most algorithms inefficient when applied to process simulations.

Many different optimization techniques have been applied to process simulators. Gradient-based optimizers have been applied using finite difference approximation for derivatives. Derivative-free optimization techniques can be applied, but many rely prohibitively large numbers of objective function evaluations without extensive parallelization [2]. One approach to mitigate the challenges of expensive black-box optimization is to approximate the objective and constraint functions with surrogate models. In theory, these types of optimization algorithms should improve in accuracy each time the objective and constraint functions are sampled, learning characteristics of the problem each iteration [3].

Several types of surrogate models have been used to approximate process simulators. Automatic surrogate model generation has been achieved through several routes. ALAMO uses subset selection for constrained regression to generate algebraic models suitable for optimization [4–6]. Others have used parametric [7] and nonparametric regression methods like neural networks [8], radial basis functions [9], and kriging models [10–12] to approximate process simulations.

The Efficient Global Optimization (EGO) algorithm [13] is a prevalent example of surrogate-based optimization. EGO uses a kriging surrogate model in an inner loop optimization to pick the next point to sample. While it has been extensively used in aerospace engineering design

optimization, EGO has rarely been applied to process engineering systems.

Contemporary research studies probability of feasibility, mean kriging predictions, and lower confidence bounds to constrain EGO's inner loop [14, 15]. This work applies EGO with selected constraint approaches to a post-combustion carbon capture process modeled in ProMax®. The objective is to minimize process energy intensity subject to process and reliability constraints.

The results compare the merits of each constraint approach according to constraint faithfulness, final objective value, and solution reliability. Conclusions are drawn to recommend which methods are most effective for the post-combustion carbon capture process.

CONSTRAINED EGO OVERVIEW

EGO was first published by Jones, Schonlau, and Welch in 1998 [13]. They developed the algorithm to globally optimize expensive objective functions. The overall structure of the algorithm is as follows. Let $F(x)$ be function of independent variables x to be minimized that returns a value y. $F(x)$ can be sampled at different points $X = \{x_1, x_2, \dots, x_n\}$ yielding $Y = \{y_1, y_2, \dots, y_n\}$. This initial dataset is selected using methods called design of experiments to fill the search space. X and Y are used to generate a kriging model f with mean and variance functions. Equation 1 shows the structure of the kriging model used in this work where β_i and θ_l are sets of hyperparameters tuned during the model building process.

$$\hat{\mu}(\mathrm{x}) = \sum_{i=1}^{n} \beta_i \, y_i + \prod_{l=1}^{n} \exp\left(-\theta_l \left|x_l^{(i)} - x_l^{(j)}\right|\right) \quad (1)$$

EGO uses this predicted mean and a predicted variance within selection criteria to determine the next best point to evaluate using the actual objective function. EGO has traditionally maximized a property called expected improvement EI to select the next point to evaluate. The expected improvement function is written in equation 2, where $\sigma(\mathrm{x})$ is the prediction standard deviation, and Φ and ϕ are the cumulative and probability density functions, respectively.

$$EI(x) = \left(f_{\min} - \hat{\mu}(\mathrm{x})\right) \Phi(a(\mathrm{x})) + \sigma(\mathrm{x}) \phi(a(\mathrm{x})) \quad (2)$$

$$a(x) = \frac{f_{\min} - \hat{\mu}(\mathrm{x})}{\sigma(\mathrm{x})}$$

Once EGO determines the point that maximizes the expected improvement function, it samples the objective function with the point. The new sampled point is then added to the end of the dataset. As shown in Figure 1, the next iteration then begins by refitting the kriging model with the new dataset.

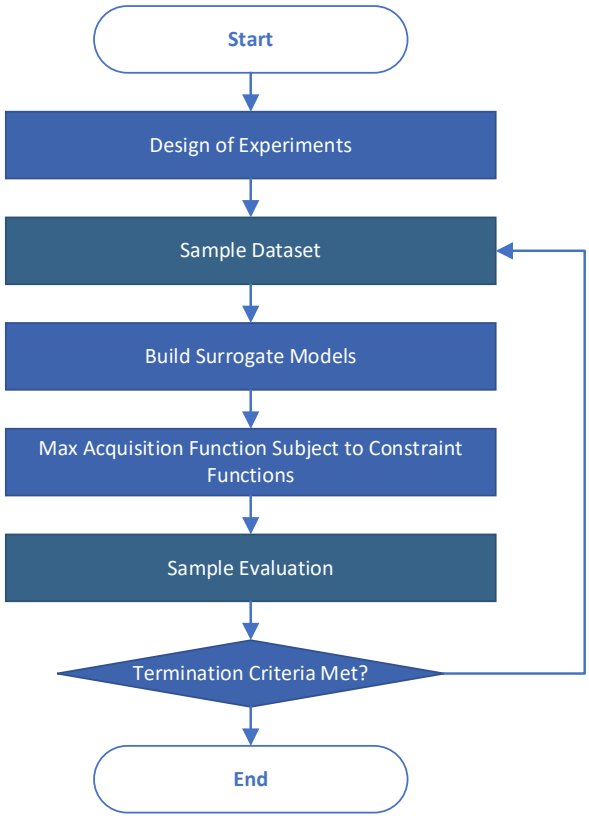

Figure 1. General EGO Algorithm Flowchart

Several constraint-handling methods have been developed for EGO. Modifying the next point selection criteria, the three approaches tested in this work rely on different properties of kriging models to enforce constraint boundaries. Two of these methods rely on a calculated probability of feasibility and were proposed by Sohst et al [14], who found that each method had its merits solving both mathematical test problems and aerodynamic shape optimization. Probability of feasibility can be conceptually understood as the probability that each constraint will be satisfied for a point based on the uncertainty in the kriging model for each constraint function. The formulation is shown in equation 3 where the constraint function is written in the form $g(x) \leq 0$. Overall probability of feasibility is just the product of each individual constraint's probability of feasibility.

$$PF(x) = \Phi\left(-\frac{\hat{g}(x)}{\sigma(\mathrm{x})}\right) \quad (3)$$

Probability of feasibility can be used in a few different ways to augment expected improvement within EGO's next point selection criteria. In one method, the product of expected improvement and probability of feasibility is maximized to select the next sample point. This method will be referred to as OFPF (Objective Function x Probability of Feasibility) in this work and is shown in equation 4.

$$\max OFPF(x) \quad (4)$$

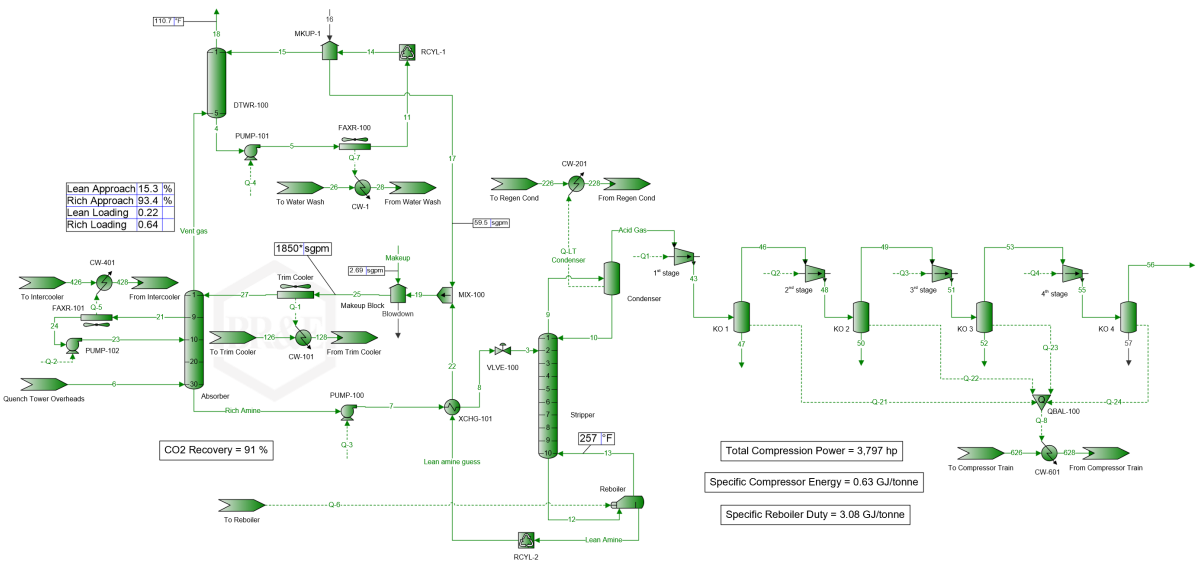

Figure 2: Post-combustion carbon capture process model with compression.

$$OFPF(x) = EI(x) \cdot PF(x)$$

Another method tested in this work applies a probability of feasibility constraint to the maximization of expected in the next point selection suboptimization problem. This method will be referred to as PFCON (Probability of Feasibility Constraint).

$$\max EI(x) \tag{5}$$

$$\text{s.t. } PF(x) \geq 0.5$$

Constraints can also be enforced using a concept called the upper trust bound (UTB) of the kriging value. Given a desired confidence interval, the kriging model can calculate an upper bound on the constraint value by adding a factor of uncertainty. This constraint on the next point selection criteria is shown in equation 7 below where the constraint must be satisfied within three standard deviations of the kriging mean.

$$\max EI(x) \tag{6}$$

$$\text{s.t. } \hat{g}(x) \leq 3\sigma(x)$$

If EGO selects a point where the objective function or constraint functions are undefined, a sufficiently suboptimal point approximating an infinite objective value can be used [16]. This approach should sufficiently penalize points in regions of the search space that cannot be evaluated.

CARBON CAPTURE PROCESS MODEL

Gas processors have used amines to recover CO_2 and H_2S from natural gas for nearly a century. After cooling the flue gas with a quench tower, the process of post-combustion carbon capture with amines contacts an aqueous amine solvent with a CO_2-rich stream to chemically absorb CO_2 with the amine. The CO_2-rich amine is then heated in a still to regenerate the amine. Figure 2 provides a process flow diagram of the example unit used in the case study.

The main difference between post-combustion carbon capture and natural gas treating lies in the partial pressure of CO_2 in the feed gas. The concentration of CO_2 in the flue gas from a natural gas power plant is about 4 mol%. While this is easily within the range of concentrations found in natural gas, the pressure of the flue gas is near atmospheric pressure. The partial pressure of CO_2 in the flue gas will be 10-100 times less than in typical natural gas amine sweetening units, leading to the differences in the design of the two processes.

Flue gas carbon capture units are marked by larger absorber columns, due to the large volume of gas, with extensive water wash sections to reduce amine losses to the atmosphere. The amine solvent lost is not only expensive but also an air pollutant. Some designs also employ a side cooler, a feature not usually afforded for natural gas treating. Cooling the amine in the absorber removes heat of reaction and shifts equilibrium towards absorption in the liquid.

The example facility in this case study has a 30 ft diameter absorber packed with 60 ft of Sulzer IMTP #50 Metal random packing solved with ProMax's Mass + Heat Transfer calculation method. The regenerator is a 9 ft diameter column modeled with 10 ideal stages of separation. The amine circulated is the CESAR-1 blend of 27 wt% amino methyl propanol (AMP) and 13 wt% piperazine.

Table 1: Inlet flue gas properties and composition

Feed Property	
Temperature	117 °F
Pressure	2.5 psig
Standard Vapor Volumetric Flow	406 MMSCFD
Feed Composition	**mol %**
Carbon Dioxide	3.99
Nitrogen	75.03
Oxygen	11.97
Water	9.00

Operators control the plant by manipulating the amine circulation rate, water wash rate, and reboiler duty. Operators are economically incentivized to minimize energy use while achieving a CO_2 recovery greater than 90% and amine losses below a permitted threshold. Utilities are integrated with the power generation facility. The amine reboiler can be powered by a slipstream of low-pressure steam from the heat recovery network of the powerplant. When integrated into the low-pressure steam circuit, the steam dedicated to the reboiler singlehandedly reduces net power generation from 100 MW to 87 MW for the base-case simulation. Pumps and compressors can be powered by electricity generated onsite.

Table 2: Base carbon capture model power use summary.

Unit Operation	**Power**
Gas turbine	68 MW
Steam turbines (no CC)	32.7 MW
Total power production	**100.7 MW**
Reboiler steam power reduction	-12.8 MW
Flue gas blower	-5.1 MW
Amine and process water pumps	-0.1 MW
CO_2 Compression Power	-2.8 MW
Cooling water pumps	-0.6 MW
Total power usage	**-21.4 MW**
Net power production	**79.3 MW**

The desired CO_2 recovery depends on several factors including but not limited to local laws, plant scale, CO_2 sequestration or utilization strategy, and investor pressures. For plants located in the United States, the IRS's Section 45Q tax credit for carbon sequestration credits a dollar per ton amount based on the ultimate CO_2 use for eligible facilities [17]. In 2023 for new non-direct air capture processes, 45Q credits up to is $85/tonne for geologically sequestered CO_2 and $60/tonne for other qualified uses of CO_2 for the first 12 years of operation. Eligible power plants must capture at least 18,750 tonnes of CO_2 and be designed to capture at least 75% of the plant's emissions. In practice, many of these facilities are designed to capture at least 90% of baseline CO_2 emissions.

Once CO_2 is captured, it will require compression for transportation and its ultimate use. CO_2 transmission lines are designed to operate over 1000 psig in the so called supercritical "dense phase" where the fluid can be effectively pumped like a liquid. In this case, the captured CO_2 leaves the facility at 1500 psig.

OPTIMIZATION FORMULATION

The implementation of constrained EGO uses the Surrogate Modeling Toolbox [18] package in Python. SMT includes an unconstrained implementation of EGO that was augmented to generate kriging models of each constraint function and use PFCON, UTB, and OFPF as next point selection criteria. The formulations used for next point selection criteria are described in equations (4) – (6) previously. These formulations are solved using a python SLSQP implementation [19] from 20 different starting points.

Any simulation run that did not converge in ProMax was given an objective value of 10 GJ/tonne, which was far greater than any observed objective value. Constraints for these unconverged samples were given values of 10 in standard form ($g(x) \leq 0$) to denote a violation of each constraint.

The first task for developing an optimization formulation for a process is determining the most appropriate objective function and the most necessary constraints. For post-combustion carbon capture on power plant flue gas, one useful objective function is to minimize the energy used for carbon capture. Likely all this energy will be supplied by the power plant, so minimizing energy consumption will minimize the impact of carbon capture on plant profitability.

The overwhelming power requirement in the carbon capture process is the heat used to drive the reboiler. Of the power requirements shown in Table 2, the only significant costs that could be affected by the carbon capture unit itself are the reboiler duty and compression power. To avoid penalizing higher CO_2 recovery inherently, the objective function $\hat{E}(x)$ will be the sum of the energy consumed by both the CO_2 compressors and the reboiler duty per unit of recovered CO_2 in units of GJ/tonne CO_2.

Constraints are selected to ensure that equipment and operating constraints are met. The facility will be required to exceed 90% CO_2 recovery $C(x)$, emit less than 300 tonne/yr of amine solvent $S(x)$, and not exceed a calculated 95% fraction flooding in both the absorber $F_a(x)$ and stripper $F_s(x)$.

Decision variables are limited to properties under operational control, leaving amine circulation a, water wash circulation w, and reboiler duty as candidates. In this study, the lean loading l, defined as the molar ratio of CO_2 and amine in the amine entering the absorber, will

Figure 3: Comparison of objective function, expected improvement, probability of feasibility, and feasible solution progress by iteration. Missing iterations failed to yield a sample point during sample point selection.

be used as a decision variable since it lends itself better to linear bounds than reboiler duty and should be more independent of other decision variables.

$$\begin{aligned} &\min \hat{E}(x) \text{ where } x = (a, w, l) \\ &\text{subject to} \quad C(x) \geq 90\% \\ &\qquad\qquad \mathrm{S}(x) \leq 300 \text{ tonne/yr} \\ &\qquad\qquad F_a(x),\ F_s(x) \leq 95\% \\ &\qquad\qquad 1500 \leq a \leq 3000 \\ &\qquad\qquad 3000 \leq w \leq 5000 \\ &\qquad\qquad 0.05 \leq l \leq 0.2 \end{aligned} \tag{8}$$

Each constraint function is passed to the algorithm in the form $g(x) \leq 0$. A Latin hypercube design of experiments is used to sample 30 points. This initial dataset becomes training points for the first kriging model. Next, each constraint-handling method is allowed 20 objective function evaluations to evaluate the search space and find an optimal solution.

One familiar with amine units would expect lower amine circulation rates and higher lean loadings to result in lower objective values. While the heat of absorption per ton of CO_2 is effectively constant in this system, heating more solvent to the temperature required to desorb CO_2 requires extra heat. One would also expect the water wash circulation should converge to the minimum required to meet the amine loss constraint.

RESULTS AND DISCUSSION

The performance of each constraint method is evaluated using three criteria: constraint faithfulness, solution reliability, and best optimal solution. For this case study, each constraint method provides a feasible solution, but none of the methods reliably converged in the allotted number of iterations.

Objective function values for each iteration are shown in Figure 3. Optimal solutions for each run, plus the best solution observed for the problem in the study are stated in Table 3. This best solution was found by

chance in the initial design of experiments. The most optimal solutions had an intermediate value of lean loading between 0.12 – 0.15 mol CO_2/mol amine which allowed lower circulation rates to meet the 90% CO_2 recovery constraint.

Table 3: EGO optimal solutions by constraint method.

	PFCON	UTB	OFPF	Best
Optimal Solution (GJ/tonne)	3.56	3.52	3.50	3.418
Amine Flow (sgpm)	1722	1626	1586	1575
Water Wash Flow (sgpm)	3976	4596	4421	4367
Lean Loading (mol/mol)	0.189	0.139	0.120	0.146

Despite not converging on a consistent operating point, the solutions provided by each method favor the expected minimal amine circulation rate. What was not expected was the extent to which lower lean loadings were preferred. Contacting flue gas with leaner than the maximum required lean loading to achieve 90% CO_2 recovery increased the capacity of each gallon of amine in circulation enough to offset the increased regeneration energy per gallon of amine. This resulted in lower energy requirements per metric ton of CO_2 captured.

Further analysis on the objective function values showed that specific compression power was effectively constant at about 0.63 GJ/tonne CO_2 captured. This indicates that compression power per unit of CO_2 captured was unaffected by regenerator operation while the overhead pressure was held constant.

Table 4: EGO run characteristics by constraint method.

	PFCON	UTB	OFPF
Failed Iterations	12	1	0
Feasible Points	4	4	8
Infeasible Points	4	15	12
Simulator Execution Error	0	6	2

Table 4 shows the incident rate of sample point selection failures and the tendency of each method to generate feasible solutions. OFPF produced the best optimal solution and the most feasible points with the least inner-loop failures. PFCON rarely converged to a sample point with its inner-loop optimization; however, when a sample point was selected, it had the highest rate of feasible sample points. UTB constraints rarely selected feasible points, and frequently sampled points where the simulator could not converge to a solution. These trends observed between the different constraint methods are consistent with the conclusions of Sohst et al [14].

CONCLUSIONS

Each of the three tested constraint-handling methods yielded a feasible optimal solution; however, none of these methods were able to converge on an optimum or surpass a solution found in the design of experiments in the allowed number of iterations.

OFPF resulted in the best optimal solution found and had the lowest incidence of failures to select a new sample point. Finding a similar solution to OFPF, UTB sampled far more infeasible points than any of the other algorithms. PFCON suffered from several incidences where the next point selection algorithm failed to yield a sample point. However, when a sample point was determined, PFCON was the most likely to yield a feasible solution. The numerical issues of PFCON could be addressed by modifying the implementation of EGO used.

One potential improvement is to replace the multi-start SLSQP optimization algorithm to find the next sample point. The expected improvement objective function is highly multimodal and evaluates very quickly, lending itself well to heuristic optimization methods that would fight through local minima more effectively.

The effects of different constraint parameter values and larger numbers of EGO iterations on algorithm performance were not studied. More iterations could result in convergence to a better solution. There is a chance that different lower bound for probability of feasibility in PFCON would improve its reliability. Future work could compare parameters for each constraint method on different types of functions over more iterations.

Ultimately, applying these optimization methods to a chemical process simulator produced similar results to previous work on aerodynamic shape optimization. Further improvements on the algorithm would be necessary for constrained EGO to be of practical use for optimizing process simulations.

ACKNOWLEDGEMENTS

The authors acknowledge Bryan Research & Engineering, LLC for providing the resources to conduct this work.

REFERENCES

1. Elbashir, N.O., El-Halwagi, M.M., Economou, I.G., Hall, K.R.: Natural Gas Processing from Midstream to Downstream. Wiley (2018).
2. Vu, K.K., D'Ambrosio, C., Hamadi, Y., Liberti, L.: Surrogate-based methods for black-box optimization. Int. Trans. Oper. Res. 24, 393–424 (2017).
3. Pardalos, P.M., Rasskazova, V., Vrahatis, M.N. eds: Black Box Optimization, Machine Learning, and No-

Free Lunch Theorems. Springer International Publishing, Cham (2021).
4. Cozad, A., Sahinidis, N.V., Miller, D.C.: Learning surrogate models for simulation-based optimization. AIChE J. 60, 2211–2227 (2014).
5. Wilson, Z.T., Sahinidis, N.V.: The ALAMO approach to machine learning. Comput. Chem. Eng. 106, 785–795 (2017).
6. Ma, K., Sahinidis, N.V., Amaran, S., Bindlish, R., Bury, S.J., Griffith, D., Rajagopalan, S.: Data-driven strategies for optimization of integrated chemical plants. Comput. Chem. Eng. 166, 107961 (2022).
7. Brambilla, A., Vaccari, M., Pannocchia, G.: Analytical RTO for a critical distillation process based on offline rigorous simulation. IFAC-Pap. 55, 143–148 (2022).
8. Thon, C., Finke, B., Kwade, A., Schilde, C.: Artificial Intelligence in Process Engineering. Adv. Intell. Syst. 3, 2000261 (2021).
9. Regis, R.G.: A Survey of Surrogate Approaches for Expensive Constrained Black-Box Optimization. In: Le Thi, H.A., Le, H.M., and Pham Dinh, T. (eds.) Optimization of Complex Systems: Theory, Models, Algorithms and Applications. pp. 37–47. Springer International Publishing, Cham (2020).
10. Palmer, K., Realff, M.: Metamodeling Approach to Optimization of Steady-State Flowsheet Simulations. Chem. Eng. Res. Des. 80, 760–772 (2002).
11. Palmer, K., Realff, M.: Optimization and Validation of Steady-State Flowsheet Simulation Metamodels. Chem. Eng. Res. Des. 80, 773–782 (2002).
12. Caballero, J.A., Grossmann, I.E.: An algorithm for the use of surrogate models in modular flowsheet optimization. AIChE J. 54, 2633–2650 (2008).
13. Jones, D.R., Schonlau, M., Welch, W.J.: Efficient Global Optimization of Expensive Black-Box Functions. J. Glob. Optim. 13, 455–492 (1998).
14. Sohst, M., Afonso, F., Suleman, A.: Surrogate-based optimization based on the probability of feasibility. Struct. Multidiscip. Optim. 65, 10 (2022).
15. Durantin, C., Marzat, J., Balesdent, M.: Analysis of multi-objective Kriging-based methods for constrained global optimization. Comput. Optim. Appl. 63, 903–926 (2016).
16. Audet, C., Caporossi, G., Jacquet, S.: Binary, unrelaxable and hidden constraints in blackbox optimization. Oper. Res. Lett. 48, 467–471 (2020).
17. Jones, A.C., Marples, D.J.: The Section 45Q Tax Credit for Carbon Sequestration. Congressional Research Service (2023).
18. Saves, P., Lafage, R., Bartoli, N., Diouane, Y., Bussemaker, J.H., Lefebvre, T., Hwang, J.T., Morlier, J., Martins, J.R.R.A.: SMT 2.0: A Surrogate Modeling Toolbox with a focus on Hierarchical and Mixed Variables Gaussian Processes. ArXiv Prepr. (2023).
19. Virtanen, P., Gommers, R., Oliphant, T.E., Haberland, M., Reddy, T., Cournapeau, D., Burovski, E., Peterson, P., Weckesser, W., Bright, J., van der Walt, S.J., Brett, M., Wilson, J., Millman, K.J., Mayorov, N., Nelson, A.R.J., Jones, E., Kern, R., Larson, E., Carey, C.J., Polat, İ., Feng, Y., Moore, E.W., VanderPlas, J., Laxalde, D., Perktold, J., Cimrman, R., Henriksen, I., Quintero, E.A., Harris, C.R., Archibald, A.M., Ribeiro, A.H., Pedregosa, F., van Mulbregt, P., SciPy 1.0 Contributors: SciPy 1.0: Fundamental Algorithms for Scientific Computing in Python. Nat. Methods. 17, 261–272 (2020).